Available online at www.sciencedirect.com
ScienceDirect
International Journal of Heat and Fluid Flow 29 (2008) 545–556
International Journal of HEAT AND FLUID FLOW
www.elsevier.com/locate/ijhff

Fully developed mixed convection in horizontal and inclined tubes with uniform heat flux using nanofluid

M. Akbari [a], A. Behzadmehr [a,*], F. Shahraki [b]

[a] Mechanical Engineering Department, Zahedan, Iran
[b] Nanotechnology Institute, University of Sistan and Baluchestan, Zahedan, Iran

Received 30 May 2007; received in revised form 25 October 2007; accepted 27 November 2007
Available online 22 January 2008

Abstract

Fully developed laminar mixed convection of a nanofluid consists of water and Al_2O_3 in horizontal and inclined tubes has been studied numerically. Three-dimensional elliptic governing equations have been solved to investigate the flow behaviors over a wide range of the Grashof and Reynolds numbers. Comparisons with previously published experimental and numerical works on mixed convection in a horizontal and inclined tube are performed and good agreements between the results are observed. Effects of nanoparticles concentration and tube inclinations on the hydrodynamics and thermal parameters are presented and discussed. It is shown that the nanoparticles concentration does not have significant effects on the hydrodynamics parameters. Heat transfer coefficient increases by 15% at 4 Vol.% Al_2O_3. Skin friction coefficient continually increases with the tube inclination, but the heat transfer coefficient reaches a maximum at the inclination angle of 45°.

Keywords: Laminar mixed convection; Nanofluid; Buoyancy force; Horizontal tube; Inclined tubes

1. Introduction

Fluids are essential for heat transfer in many engineering equipments. Low thermal conductivity of conventional heat transfer fluids such as water, oil, and ethylene glycol mixture is a serious limitation in improving the performance and compactness of these engineering equipments. To overcome this disadvantage, there is strong motivation to develop advanced heat transfer fluids with substantially higher conductivity. One way is to adding small solid particles in the fluid. Maxwell (1873) showed the possibility of increasing thermal conductivity of a mixture by more volume fraction of solid particles. The particles with micrometer or even millimeter dimensions were used. Those particles caused several problems such as abrasion, clogging and additional pressure drop. By improving the technology to make particles in nanometer dimensions, a new generation of solid–liquid mixtures that is called nanofluid, was appeared. The nanofluids are a new kind of heat transfer fluid containing small quantity of nano-sized particles (usually less than 100 nm) that are uniformly and stably suspended in a liquid. The dispersion of a small amount of solid nanoparticles in conventional fluids changes their thermal conductivity remarkably. Estman et al. (2001) quantitatively analyzed some potential benefits of nanofluids for augmenting heat transfer and reducing size, weight and cost of thermal apparatuses, while incurring little or no penalty in the pressure drop.

Researchers have demonstrated that oxide ceramic nanofluids consisting of CuO or Al_2O_3 nanoparticles in water or ethylene glycol exhibit enhanced thermal conductivity (Lee et al., 1999). For example, using Al_2O_3 particles having a mean diameter of 13 nm at 4.3% volume fraction increased the thermal conductivity of water under stationary conditions by 30% (Masuda et al., 1993). On the other hand, larger particles with an average diameter of 40 nm led to an increase of less than 10% (Lee et al., 1999).

* Corresponding author. Tel.: +98 541 2446251; fax: +98 541 2447092.
E-mail address: behzadmehr@hamoon.usb.ac.ir (A. Behzadmehr).

0142-727X/$ - see front matter © 2007 Elsevier Inc. All rights reserved.
doi:10.1016/j.ijheatfluidflow.2007.11.006

Nomenclature

C_B	Boltzmann constant ($=1.38 \times 10^{-23}$ J/K)
C_f	peripherally average skin friction coefficient
C_p	specific heat (J/kg K)
D	tube diameter (m)
D_s	nanoparticle diameter (m)
g	gravitational acceleration (m s^{-2})
Gr	Grashof number $\left(=\frac{g\beta_{eff}q''D^4}{k_{eff}\upsilon_{eff}^2}\right)$
h	convection heat transfer coefficient (W/m^2 K)
k	thermal conductivity (W/m K)
Nu_m	peripherally average Nusselt number
P	pressure (pa)
Pe	Peclet number $\left(=\frac{3\pi D_S D(-dP/dZ)}{4C_B T}\right)$
q_w	uniform heat flux (W m^{-2})
r	radial direction
Re	Reynolds number $\left(=\frac{\rho_{eff}w_0 D}{\mu_{eff}}\right)$
T	temperature (K)
u	tangential velocity component (m s^{-1})
v	radial velocity component (m s^{-1})
w	axial velocity component (m s^{-1})
Z	axial direction

Greek letters

α	thermal diffusivity
β	volumetric expansion coefficient (K^{-1})
θ	angular coordinate
ϕ	volume fraction
μ	dynamic viscosity (N s m^{-2})
υ	kinematic viscosity (m^2 s^{-1})
ρ	Density (kg m^{-3})

Subscripts

b	bulk
eff	effective
f	base fluid
m	average
0	inlet condition
s	solid particles
w	wall

Furthermore, the effective thermal conductivity of metallic nanofluid increased by up to 40% for the nanofluid consisting of ethylene glycol containing approximately 0.3 vol.% Cu nanoparticles of mean diameter less than 10 nm Choi (1995).

Different concepts have been proposed to explain this enhancement in heat transfer. Xuan and Li (2000) and Xuan and Roetzel (2000) have identified two causes of improved heat transfer by nanofluids: the increased thermal dispersion due to the chaotic movement of nanoparticles that accelerates energy exchanges in the fluid and the enhanced thermal conductivity of nanofluids. On the other hand (Keblinski et al., 2002) have studied four possible mechanisms that contribute to the increase in nanofluid heat transfer: Brownian motion of the particles, molecular-level layering of the liquid/particle interface, heat transport in the nanoparticles and nanoparticles clustering. Similarly to Wang et al. (1999), they showed that the effects of the interface layering of liquid molecules and nanoparticles clustering could provide paths for rapid heat transfer. Numerous theoretical and experimental studies have been conducted to determine the effective thermal conductivity of nanofluids. However, studies show that the measured thermal conductivity of nanofluids is much larger than the theoretical predictions (Choi et al., 2001). Many attempts have been made to formulate efficient theoretical models for the prediction of the effective thermal conductivity, but there is still a serious lack in this domain (Xue, 2003; Xuan et al., 2004).

As nanofluids are rather new, relatively few theoretical and experimental studies have been reported on convective heat transfer coefficients in confined flows. Pak and Cho (1998) and Xuan and Li (2000, 2003) obtained experimental results on convective heat transfer for laminar and turbulent flow of a nanofluid inside a tube. They produced the first empirical correlations for the Nusselt number using nanofluids composed of water and Cu, TiO_2 and Al_2O_3 nanoparticles. Their results indicate a remarkable increase in heat transfer performance over the base fluid for the same Reynolds number.

Despite the fact that nanofluid is a two phase mixture, since the solid particles are very small size they are easily fluidized and can be approximately considered to behave as a fluid (Xuan and Li, 2000). Therefore, considering the ultrafine and low volume fraction of the solid particles, it might be reasonable to treat nanofluid as single phase flow in certain conditions (Yang et al., 2005). As this approach is simpler to use several theoretical studies were done based on this approach (Maiga et al., 2004; Khanafer et al., 2003; Koo and Kleinstreuer, 2005; Akbarinia and Behzadmehr, 2007). Mixed convection in inclined tubes appears in many industries such as heat exchangers, and solar energy collectors. Buoyancy force has an important role on the hydrodynamic and thermal behaviors of a fluid flow throughout the ducts. In horizontal tubes, buoyancy force appears perpendicular to the tube axis (vertical direction) and creates a secondary flow. However, in vertical tubes buoyancy force is parallel to the tube length and accelerates the near wall axial velocity. Therefore, the secondary flow does not occur and the fluid flow is accelerated by the buoyancy force at the near wall region (Behzadmehr et al., 2003). In inclined tubes gravity has two components; one in axial direction and the other perpendicular to the tube axis. Therefore, in such geometrical configurations from one hand the buoyancy forces axially accelerates the fluid flow and from the other hand it generates the secondary flow at the tube cross section.

Compared to the vertical and horizontal tubes, published results on an inclined tube is limited. Among them, Sabbagh et al. Sabbagh et al. (1976) experimentally studied mixed convection of air flows in an inclined tube. They showed that the fully developed Nusselt number decreases with increasing the tube inclination. The same observation is also seen in the experimental results were obtained by Barozzi et al. (1985). They found that increase of the slope angle from 0 to 60 produces only a small reduction in the heat transfer rate, and can therefore be disregarded as far as practical applications are concerned. Orfi et al. (1988) numerically investigated the fully developed flow in inclined tubes with uniform heat flux. They reported an optimum inclination angle for maximizing the Nusselt number.

The present paper is studied the laminar mixed convection of a nanofluid in horizontal and inclined tubes with uniform heat flux. The effects of tube inclinations and nanoparticles concentration on the hydrodynamic and thermal parameters for different *Re–Gr* combinations are shown and discussed. Therefore, the axial velocity, secondary flow and temperature profiles for different values of the particles concentrations are presented at different tube inclinations. Also, the axial profile of the convective heat transfer coefficient and the skin friction coefficient are shown and discussed.

2. Mathematical formulation

Mixed convection of a Nanofluid consisting of water and Al_2O_3 in a long tube ($D = 0.02$ m and $Z = 1.96$ m) with uniform heat flux at the solid–liquid interface has been considered. Fig. 1 shows the geometry of the considered problem. Gravitational force is exerted in the vertical direction. Therefore, symmetry is considered about the vertical central plane and calculations have been done on one half of the cylinder. The physical properties of the fluid are assumed constant except for the density in the body force, which varies linearly with the temperature (Boussinesq's hypothesis). Dissipation and pressure work are neglected. Altrafine (<100 nm) solid particles has been considered. Therefore due to their non sediment nature, behave as single phase fluid for which the fluid phase and nanoparticles are in thermal equilibrium with zero relative velocity (Putra et al., 2003; and Daungthongsuk and Wongwises, 2007). With these assumptions the dimensional conservation equations for steady state mean conditions are as follows:

Continuity equation:

$$\frac{1}{r}\frac{\partial}{\partial\theta}(\rho_{nf}u)+\frac{1}{r}\frac{\partial}{\partial r}(\rho_{nf}rv)+\frac{\partial}{\partial z}(\rho_{nf}w)=0 \tag{1}$$

Momentum equation:

θ-component

$$\frac{1}{r}\frac{\partial}{\partial\theta}(\rho_{nf}uu)+\frac{1}{r}\frac{\partial}{\partial r}(\rho_{nf}rvu)+\frac{\partial}{\partial z}(\rho_{nf}wu)+\frac{1}{r}(\rho_{nf}uv)$$
$$=-\frac{1}{r}\frac{\partial p}{\partial\theta}+\frac{1}{r^2}\frac{\partial}{\partial\theta}\left(\mu_{nf}\frac{\partial u}{\partial\theta}\right)+\frac{\partial}{\partial r}\left(\frac{\mu_{nf}}{r}\frac{\partial(ru)}{\partial r}\right)$$
$$+\frac{2\mu_{nf}}{r^2}\frac{\partial v}{\partial\theta}+\rho_{nf}g\beta_{nf}(T_w-T)\sin\theta\cos\alpha \tag{2a}$$

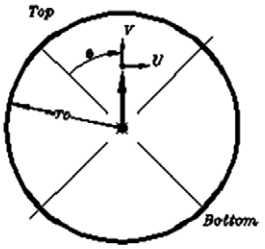

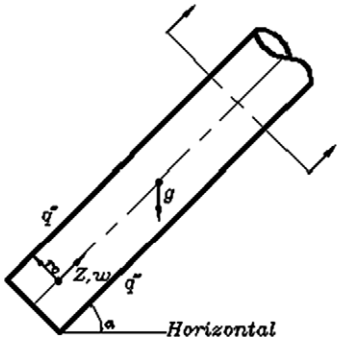

Fig. 1. Schematic of the inclined tube.

r-component

$$\frac{1}{r}\frac{\partial}{\partial\theta}(\rho_{nf}uv)+\frac{1}{r}\frac{\partial}{\partial r}(\rho_{nf}rvv)+\frac{\partial}{\partial z}(\rho_{nf}wv)-\frac{1}{r}\rho_{nf}u^2$$
$$=-\frac{1}{r}\frac{\partial p}{\partial r}+\frac{1}{r^2}\frac{\partial}{\partial\theta}\left(\mu_{nf}\frac{\partial v}{\partial\theta}\right)+\frac{\partial}{\partial r}\left(\frac{\mu_{nf}}{r}\frac{\partial(rv)}{\partial r}\right)$$
$$-\frac{2\mu_{nf}}{r^2}\frac{\partial u}{\partial\theta}-\rho_{nf}g\beta_{nf}(T_w-T)\cos\theta\cos\alpha \tag{2b}$$

z-component

$$\frac{1}{r}\frac{\partial}{\partial\theta}(\rho_{nf}uw)+\frac{1}{r}\frac{\partial}{\partial r}(\rho_{nf}rvw)+\frac{\partial}{\partial z}(\rho_{nf}ww)$$
$$=-\frac{\partial p}{\partial z}+\frac{1}{r^2}\frac{\partial}{\partial\theta}\left(\mu_{nf}\frac{\partial w}{\partial\theta}\right)+\frac{1}{r}\frac{\partial}{\partial r}\left(r\mu_{nf}\frac{\partial w}{\partial r}\right)-\rho_{nf}g\sin\alpha \tag{2c}$$

Energy equation:

$$\frac{1}{r}\frac{\partial}{\partial\theta}(\rho_{nf}uT)+\frac{1}{r}\frac{\partial}{\partial r}(\rho_{nf}rvT)+\frac{\partial}{\partial z}(\rho_{nf}wT)$$
$$=\frac{1}{r^2}\frac{\partial}{\partial\theta}\left(\frac{K_{nf}}{(C_p)_{nf}}\frac{\partial T}{\partial\theta}\right)+\frac{\partial}{r\partial r}\left(r\frac{K_{nf}}{(C_p)_{nf}}\frac{\partial T}{\partial r}\right) \tag{3}$$

The properties of nanofluid (fluid containing suspended nanoparticles) are defined as follows:

Density

$$\rho_{\text{eff}}=(1-\phi)\rho_f+\phi\rho_s \tag{4}$$

Effective thermal conductivity

$$k_{\text{eff}}=\left(\frac{k_s+(n-1)k_f-(n-1)\phi(k_f-k_s)}{k_s+(n-1)k_f+\phi(k_f-k_s)}\right)k_f \tag{5}$$

This was introduced by Hamilton and Crosser (1962). Where n is a shape factor and equal to 3 for spherical

nanoparticles. As shown by Zhang et al. (2007) this model is in good agreement with the experimental results at the low value of the nanoparticles volume fraction ($\phi < 5\%$).

Thermal diffusivity

$$\alpha_{\text{eff}} = \frac{K_{\text{eff}}}{(1-\phi)(\rho C_{\text{P}})_{\text{f}} + \phi(\rho C_{\text{P}})_{\text{s}}} \tag{6}$$

Thermal expansion coefficient (Khanafer et al., 2003)

$$\beta_{nf} = \left[\frac{1}{1+\frac{(1-\phi)\rho_{\text{f}}}{\phi\rho_{\text{s}}}}\frac{\beta_{\text{s}}}{\beta_{\text{f}}} + \frac{1}{1+\frac{\phi}{1-\phi}\frac{\rho_{\text{s}}}{\rho_{\text{f}}}}\right]\cdot\beta_{\text{f}} \tag{7}$$

Specific heat

$$(c_{\text{p}})_{nf} = \left[\frac{(1-\phi)(\rho c_{\text{p}})_{\text{f}} + \phi(\rho c_{\text{p}})_{\text{s}}}{(1-\phi)\rho_{\text{f}} + \phi\rho_{\text{s}}}\right] \tag{8}$$

Effective viscosity of water – Al_2O_3 nanofluid.

$$\mu_{nf} = (123\phi^2 + 7.3\phi + 1)\mu_{\text{f}} \tag{9}$$

which was presented by Maiga et al. (2004) for water – Al_2O_3 nanofluid based on the experimental results had been found in the literature. This equation, as compared with the Wang et al. (1999) and Lee et al. (1999), has good precision at low particles volume fractions (lower than 5%).

3. Boundary condition

This set of nonlinear elliptical governing equations has been solved subject to following boundary conditions:

– At the tube inlet ($Z = 0$):

$$w = w_0, \quad u = v = 0, \quad T = T_0 \tag{10}$$

– At the fluid-solid interface (r=D/2):

$$w = u = v = 0 \text{ and } q_{\text{w}} = -k_{\text{eff}}\frac{\partial T}{\partial r} \tag{11}$$

– At vertical symmetry plane

$$\theta = 0 \text{ and } \theta = \pi, \quad u = 0, \quad \frac{\partial v}{\partial \theta} = \frac{\partial w}{\partial \theta} = \frac{\partial T}{\partial \theta} = 0 \tag{12}$$

– At the tube outlet ($Z/D = 98$) the diffusion flux in the direction normal to the exit plane is assumed to be zero for all variables and an overall mass balance correction is applied.

4. Numerical method and validation

This set of coupled non-linear differential equations was discretized with the control volume technique. For the convective and diffusive terms second order upwind method was used while the SIMPLEC procedure was introduced for the velocity–pressure coupling. The discretization grid is uniform in the circumferential direction and non-uniform in the other two directions. It is finer near the tube entrance and near the wall where the velocity and temperature gradients are large. Several different grid distributions have been tested to ensure that the calculated results are grid independent. The selected grid for the present calculations consisted of 180, 40 and 20 nodes, respectively in the axial, radial and circumferential directions. As it shows in Fig. 2a and b, increasing the grid numbers does not significantly change centerline axial velocity and the fluid temperature, respectively along the tube length and at the fully developed region. Other axial and radial profiles are also verified to be sure the results are grid independence.

In order to demonstrate the validity and also precision of the model and the numerical procedure, calculated velocity and temperature profiles have been compared with corresponding experimental and numerical results available in the literature.

Fig. 3 shows the comparison of the calculated results with the experimental results of Barozzi et al. (1985) in horizontal and inclined tubes. The axial profile of the predicted peripherally average Nusselt number is in good agreement with the corresponding experimental results. Another comparison has also been performed with the numerical results were obtained by Choudhury and Patankar (1988). As it is shown in Fig. 4a, the concordance of the axial velocity profiles is fine. Fig. 4b compares the dimensionless temper-

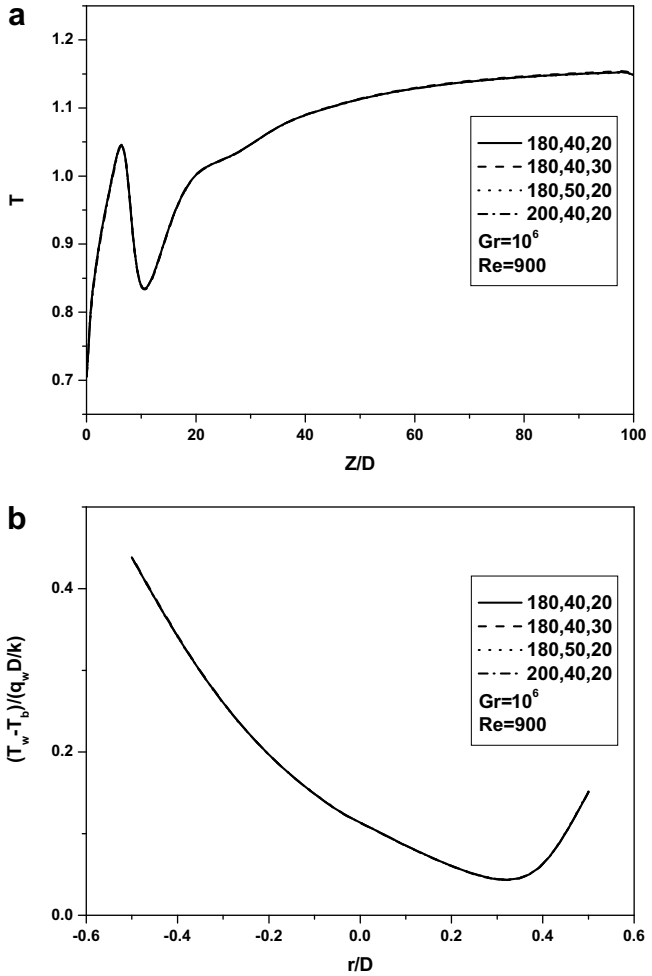

Fig. 2. Grid independence tests (a) axial profile of centerline axial velocity (b) fully developed temperature profile.

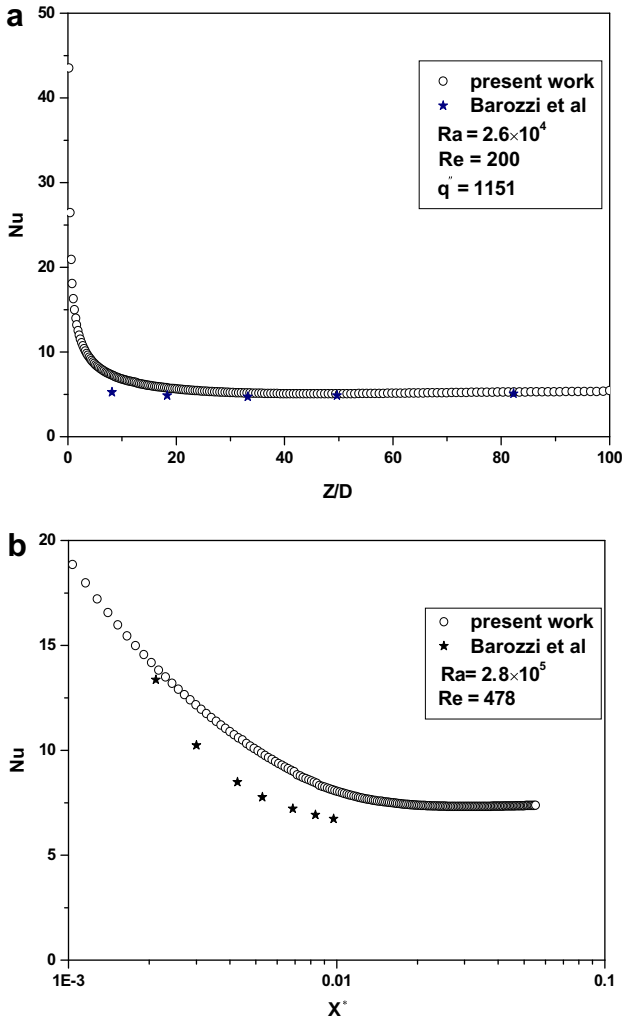

Fig. 3. Comparison of axial profile of the peripheral average Nu with experimental results of Barozzi et al. (1985) (a) horizontal tube (b) inclined tube.

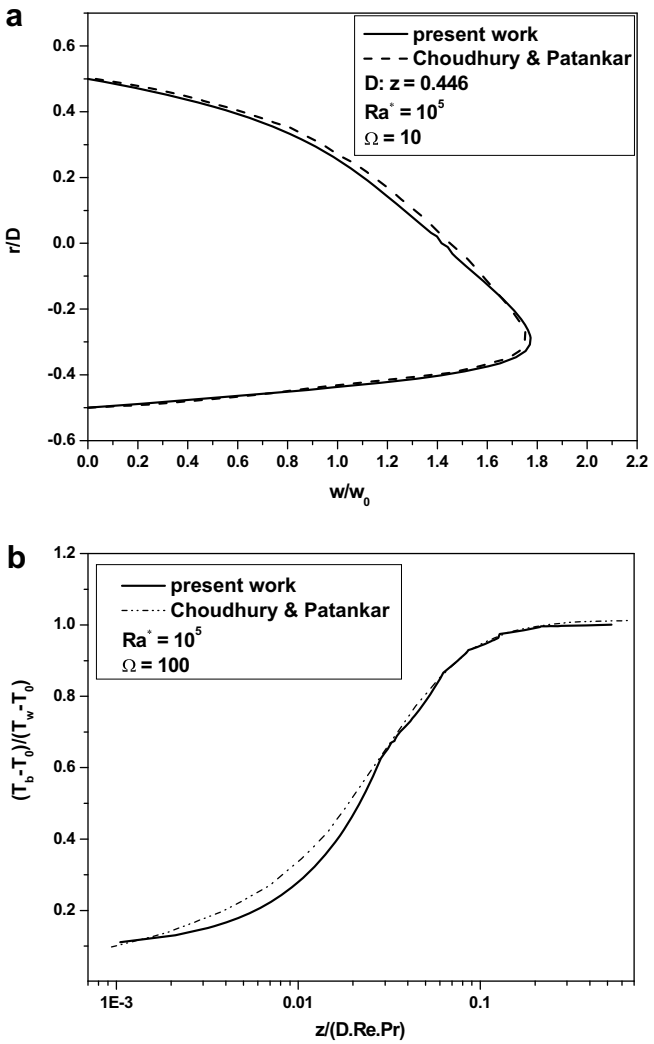

Fig. 4. Comparison with Choudhury and Patankar (1988) numerical results (a) Fully developed axial velocity (b) axial profile of temperature.

ature along the tube length. Again the results are in good agreement. Therefore the numerical procedure is reliable and can predict developing mixed convection flow in a horizontal and also an inclined tube.

5. Results and discussion

Numerical simulations have been performed over a wide range of *Re*, *Gr* and particles concentrations at five different tube inclinations. Because of similar behaviors the results are presented at $Re = 300$ for two different Grashof numbers (low and high Grashof numbers) and three different particle volume fractions (0%, 2%, 4%) on different tube inclinations. For a given Reynolds number, maximum Grashof number (or wall heat flux) are controlled for which increasing bulk temperature be lower than 40 °C. This value respects the suggested criteria for validation of the Boussinesq approximation (Nesreddine et al., 1997). These conditions also respects the situations were presented by Ding and Wen (2005) for which particles concentration could be considered uniform (very small Peclet number). The Peclet number (*Pe*) in the present conditions is less than 0.006.

For a given *Re* and three different values of the Al_2O_3 particles volume fractions (0, 2 and 4 vol.%), vectors of dimensionless secondary flow (uD/α, vD/α) and contours of dimensionless temperature ($(T - T_0)/(q_w D/k_{eff})$) at fully developed region are presented for two Grashof numbers ($Gr = 5 \times 10^4$, $Gr = 7 \times 10^5$) at three tube inclinations(0, 45 and 75°) in Figs. 5–7. In general, the fluid rises to top of the tube and falls slowly toward the center because of buoyancy force. Therefore, a secondary flow pattern appears at the tube cross section which creates a circular cell. Its position depends on the balance of the buoyancy force and the inertia of the secondary flow at the vertical plane (symmetry plane). Increasing the tube inclinations makes the secondary flow weaker. Since the component of the gravity in the tube cross section becomes smaller and consequently the secondary flow vectors decreases.

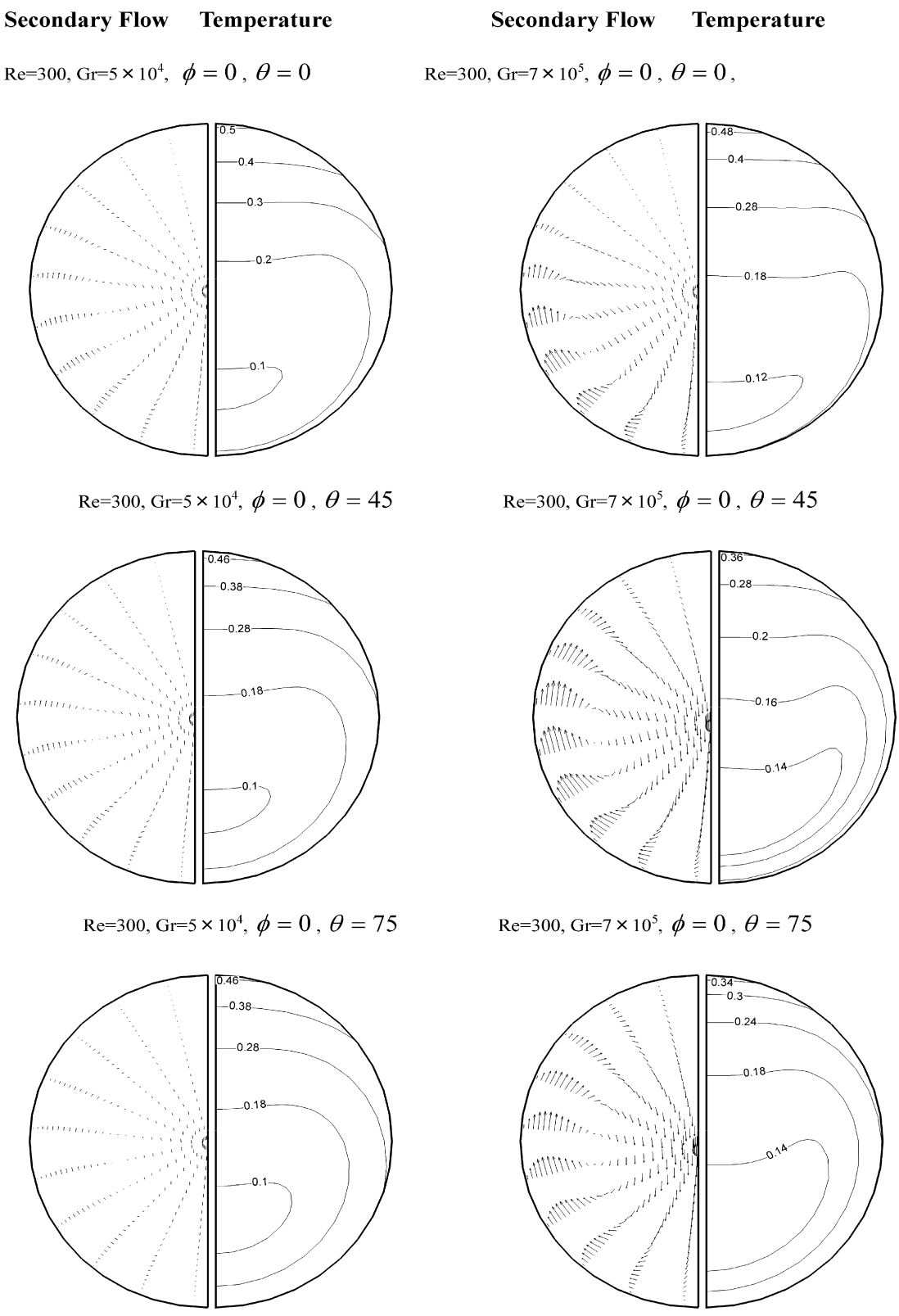

Fig. 5. Dimensionless fully developed vectors of secondary flow and contours of temperature for 0 Vol.% Al_2O_3.

Fig. 5 shows the vectors of secondary flow and also contours of temperature for pure water (zero particle concentration). The circulation cell which is appeared at the lower portion of the tube moves up by increasing the tube inclinations. As mentioned, increasing the tube inclination reduces the buoyancy forces in the tube cross section and

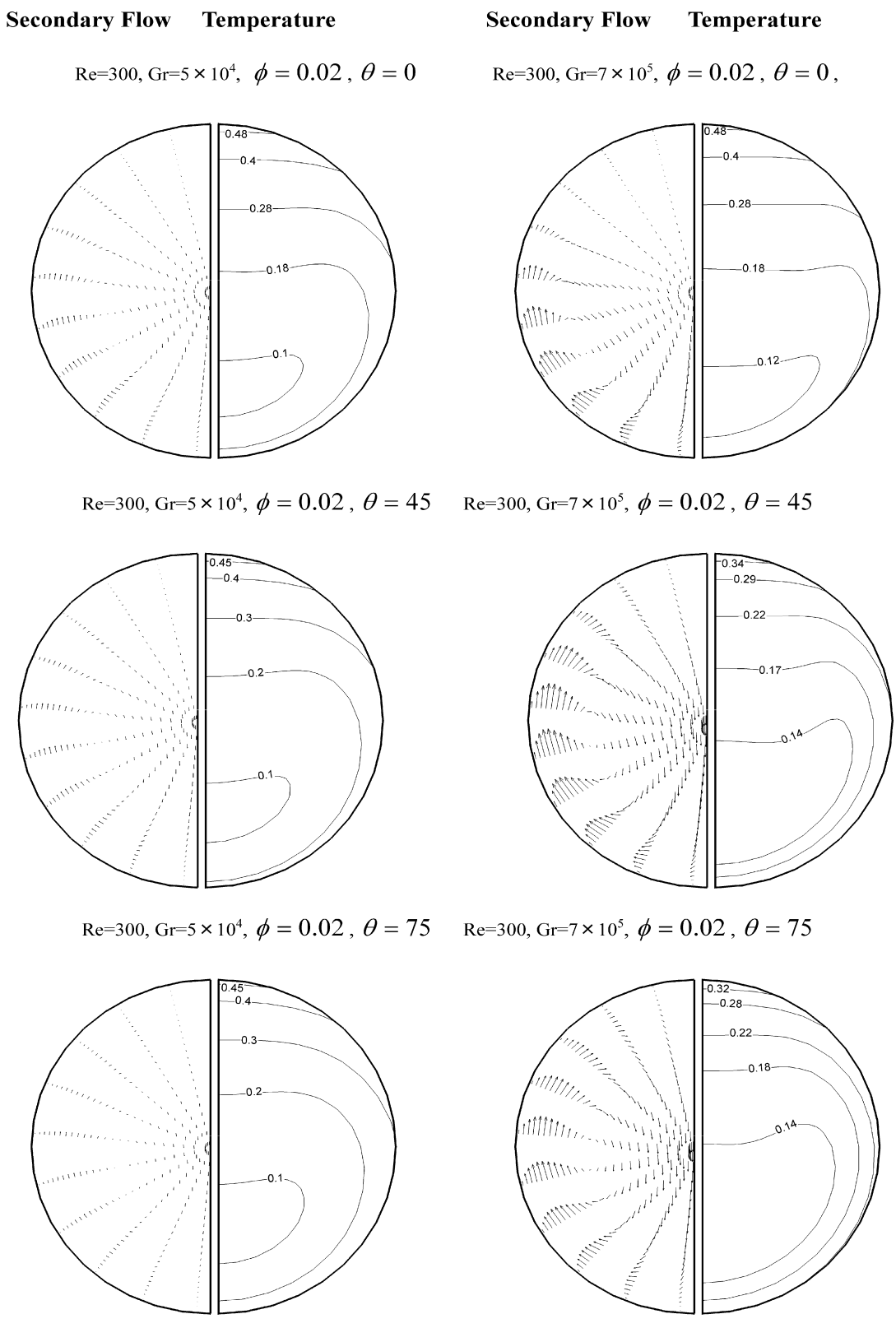

Fig. 6. Dimensionless fully developed vectors of secondary flow and contours of temperature for 2 Vol.% Al_2O_3.

so radial variation of the temperature decreases. This diminishes the inertia of the secondary flow at the vertical plane and therefore the circular cell goes up. However, increasing the Grashof number ($Gr = 7 \times 10^5$) augments the buoyancy force and stronger secondary flow is appeared. The latter causes the center of recirculation

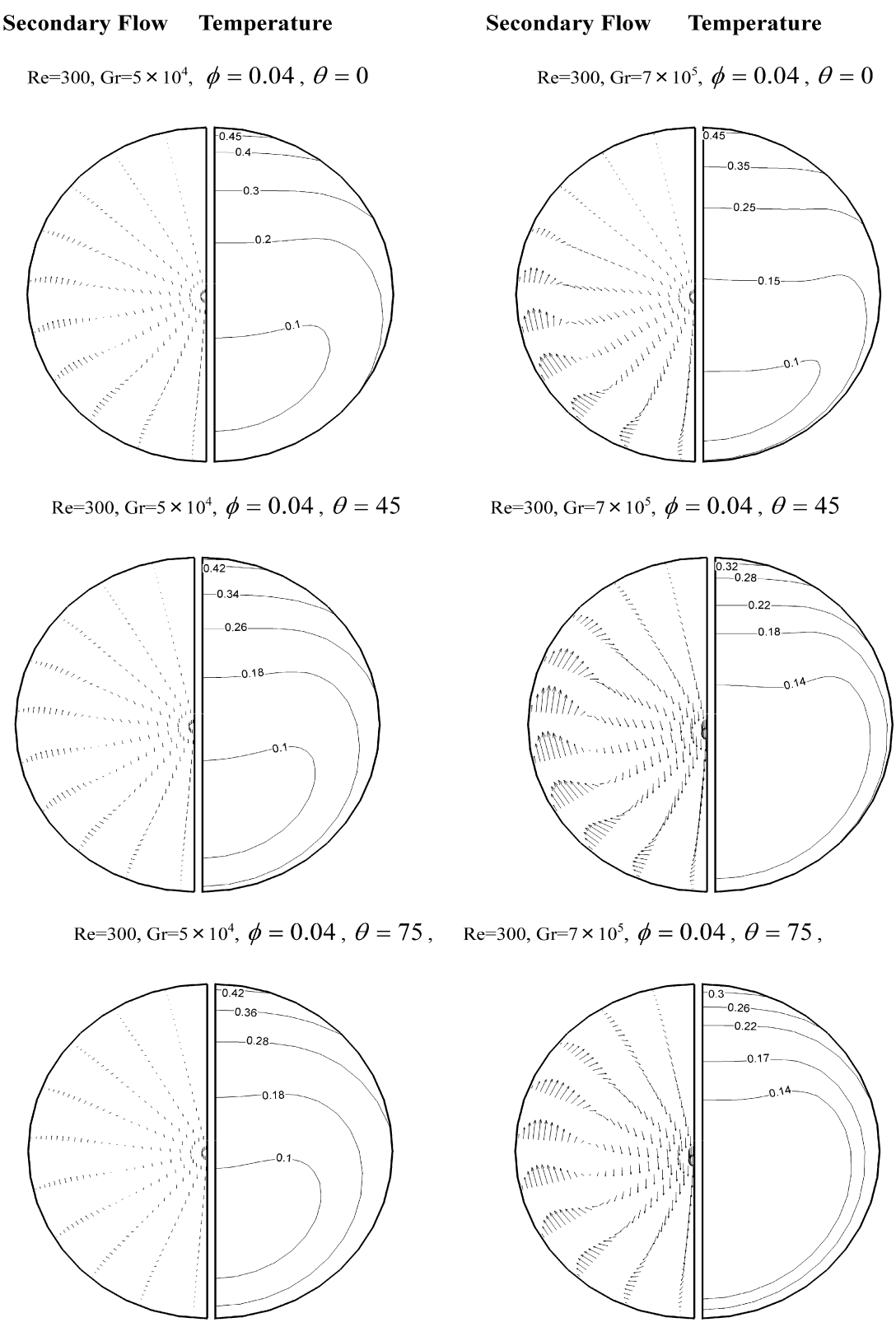

Fig. 7. Dimensionless fully developed vectors of secondary flow and contours of temperature for 4 Vol.% Al_2O_3.

backs down close to the tube wall. Such a strong secondary flow distorted the contours of temperature at the upper portion of the tube.

The effects of particles concentration on the secondary flow and temperature are shown in Figs. 6 and 7. Adding Al_2O_3 nanoparticles in water increases the effective thermal

conductivity of the fluid and therefore the molecular heat diffusion is augmented. For a given *Gr* and *Re* fluid temperature becomes more uniform by increasing particles concentration. While the secondary flow does not significantly change (despite of higher heat flux needs to keep the Grashof number constant for higher particles concentration).

Fig. 8 shows dimensionless axial velocity profile at different tube inclinations. At the lower Grashof number ($Gr = 5 \times 10^4$), secondary flow distorted axial velocity profile and its maximum value displaces toward the bottom tube's wall. Increasing the tube inclinations makes the secondary flow weaker, so the maximum value of axial velocity goes up near to the centerline. At the higher Grashof number the effect of tube inclinations becomes more evident. In the case of horizontal tube ($\theta = 0$), the maximum axial velocity appears at the lower portion of the tube. Compared to the lower *Gr*, its position approaches to the lower tube wall because of higher secondary flow. However, increasing the tube inclinations significantly changes the velocity profiles at such a high *Gr*. Increasing θ,

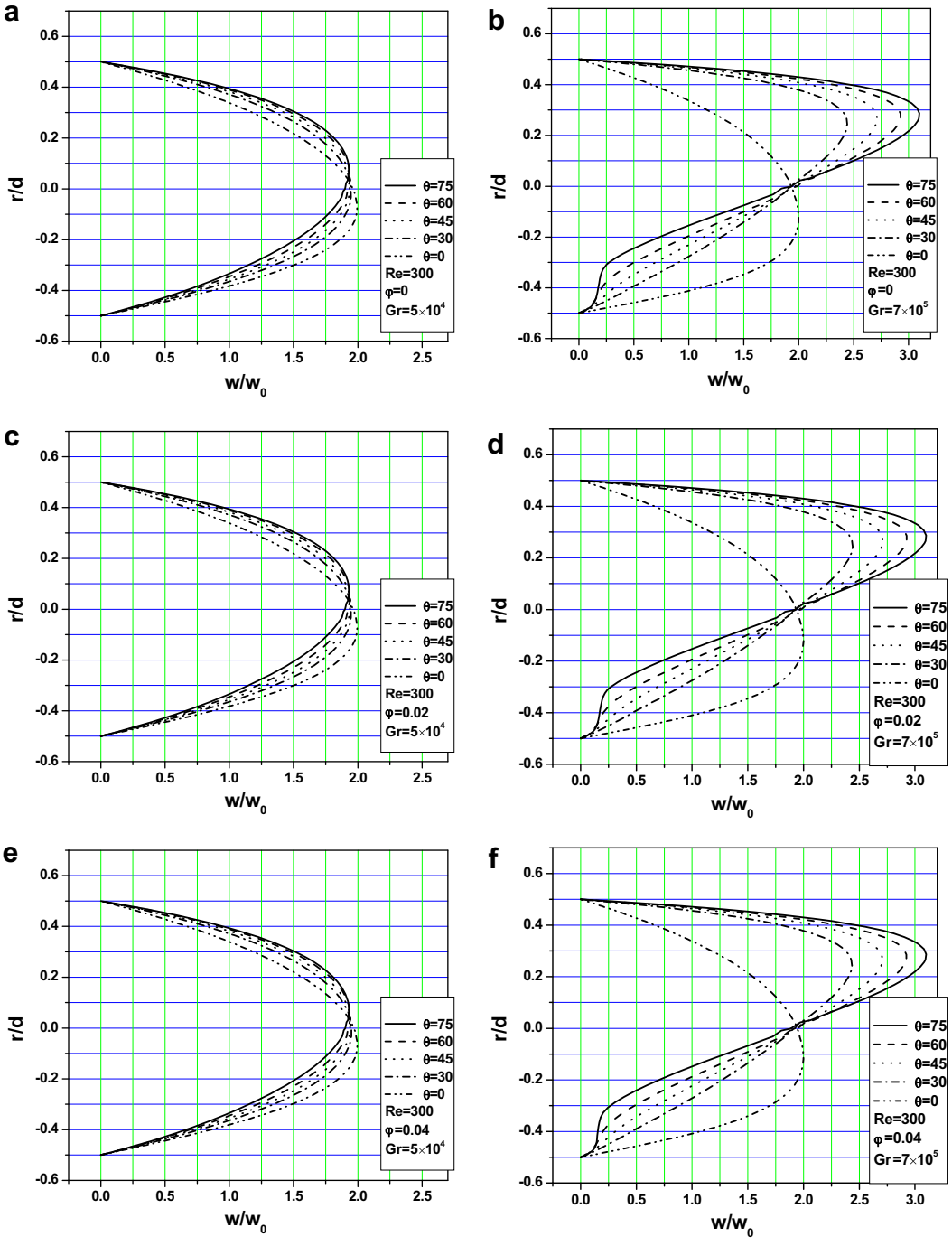

Fig. 8. Dimensionless fully developed axial velocity profiles.

augments the axial component of the buoyancy force. It accelerates the fluid flow where the fluid temperature is higher. Therefore, the maximum axial velocity approaches to the near wall region at the upper part of the tube. Fig. 8 is also shown that increasing the nanoparticles concentration does not have significant effect on the axial velocity profiles.

Axial profile of the convective heat transfer coefficient is shown in Fig. 9. At low Grashof number, h decreases and monotonically goes to its asymptotic value. In general, increasing the slope up to $\theta = 45$, the convective heat transfer coefficient augments while h is reduced by further tube inclination. Because, heat transfer enhances by two factors; the first one is the secondary flow and the second one near wall axial acceleration. The first factor is in maximum value in the horizontal tube while the highest value of the second one is in the case of vertical tube. Tube inclination, reduces the first factor and increases the second one. The balance of these two forces depends on the Reynolds number (axial momentum), Grashof number (buoyancy force)

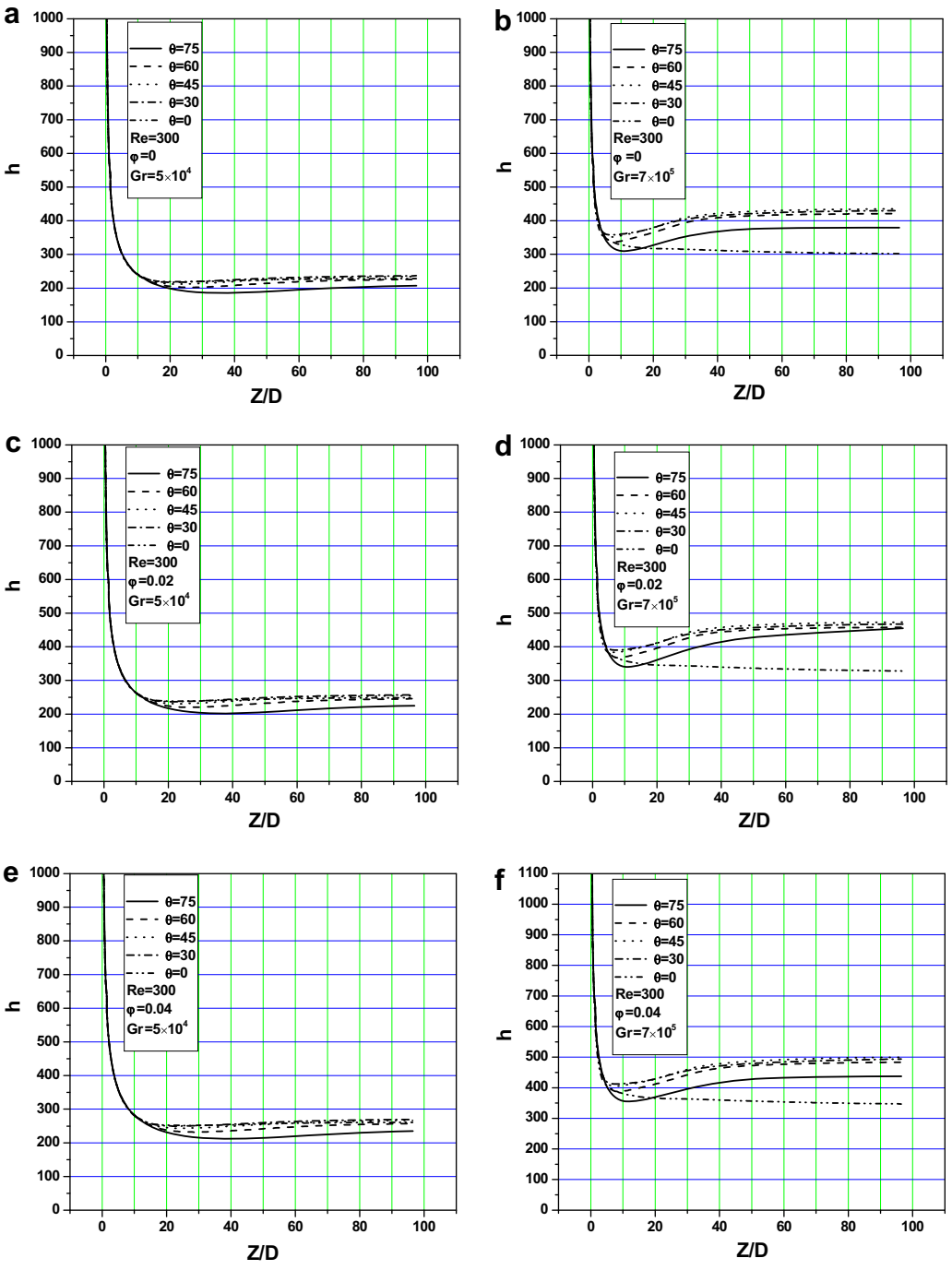

Fig. 9. Axial profile of the peripherally average convective heat transfer coefficient.

and tube inclinations. As it is clearly seen, increasing the Grashof number augments the buoyancy forces and enhances heat transfer coefficient. However, at the lower Gr, axial profile of h at the tube entrance for $\theta = 45$, is lower than the corresponding for lower tube inclinations up to $Z/D \cong 40$ while at the higher Grashof number this position becomes at $Z/D \cong 25$. At the fully developed region the highest value of h is corresponded to $\theta = 45$.

Increasing the nanoparticles concentration enhances heat transfer coefficient. This effect is more significant at $Gr = 7 \times 10^5$ for which the effect of nanoparticles is more important on the temperature profile. Nanofluid having 2 Vol.% Al_2O_3 increases 8% on the heat transfer coefficient while the corresponding enhancement for 4 Vol.% Al_2O_3 is 15%.

Fig. 10 shows the axial profile of the peripherally average skin friction coefficient. Increasing the nanoparticles volume fractions does not have significant effect on C_f. In general, increasing the tube inclinations augments the near wall flow acceleration and consequently higher skin friction occurs. This variation is more important at the higher Grashof numbers for which the buoyancy force is higher.

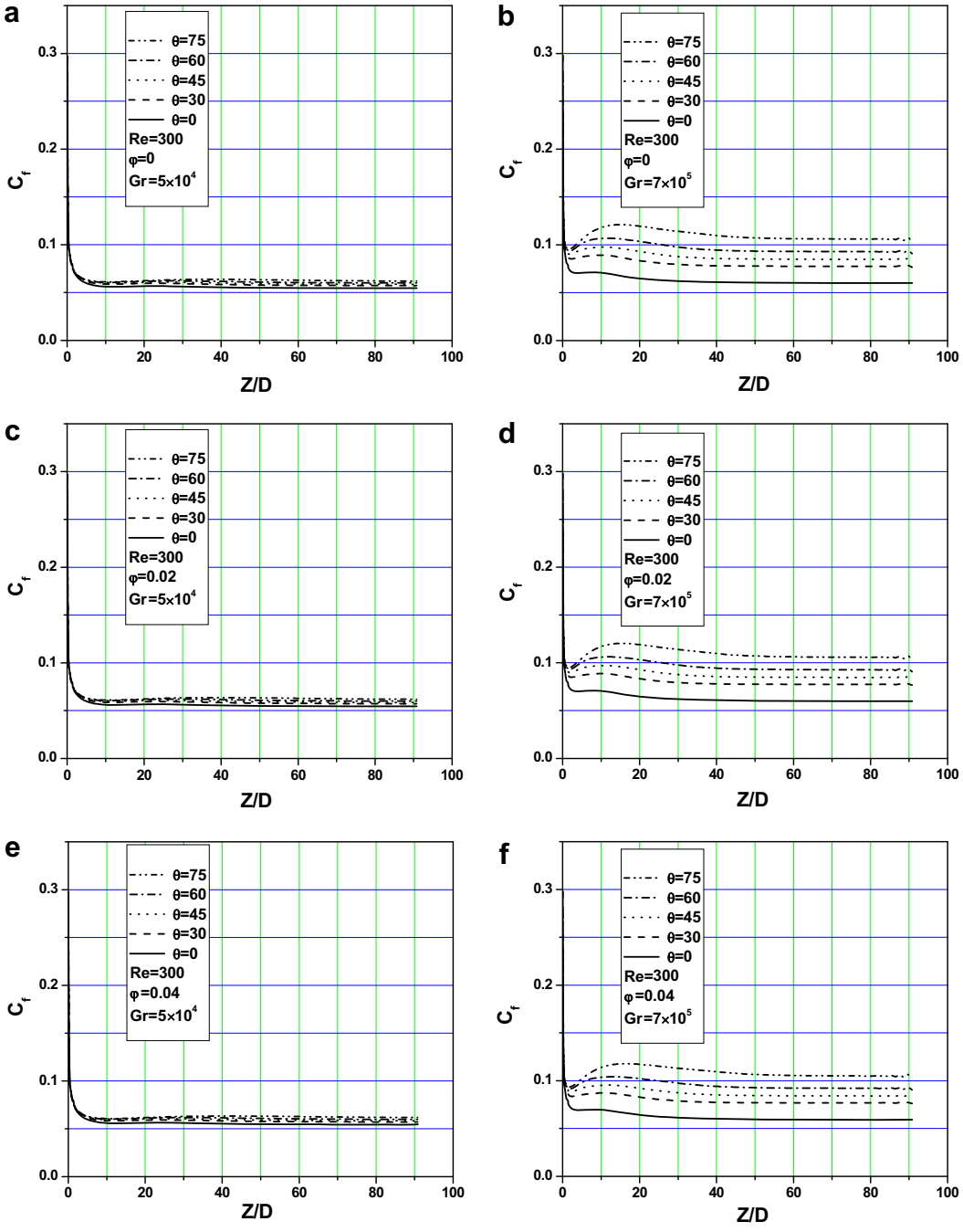

Fig. 10. Axial profile of the peripherally average skin friction coefficient.

6. Conclusion

Fully developed laminar mixed convection of a nanofluid consists of water and Al_2O_3 in horizontal and inclined tubes has been studied numerically. Three dimensional elliptic governing equations have been solved. The results illustrate that the nanoparticles concentration does not have significant effect on the secondary flow, axial velocity profile and also on the peripherally average skin friction coefficient. The fluid temperature is affected directly because of increasing molecular thermal diffusion. Heat transfer coefficient is significantly increased by 4 Vol.% Al_2O_3.

Increasing the tube inclinations, increases the axial component of the buoyancy force and reduces the corresponding component at the tube cross section. Therefore the secondary flow pattern becomes weaker and maximum axial velocity approaches to top of the tube. Skin friction coefficient is augmented by increasing the tube inclinations. However, the maximum heat transfer coefficient is achieved at $\theta = 45$.

References

Akbarinia, A., Behzadmehr, A., 2007. Numerical study of laminar mixed convection of a nanofluid in a horizontal curved tube. J. Appl. Therm. Eng. 27, 1327–1337.

Barozzi, G.S., Zanchini, E., Mariotti, M., 1985. Experimental investigation of combined forced and free convection in horizontal and inclined tubes. Meccanica 20, 18–27.

Behzadmehr, A., Galanis, N., Laneville, A., 2003. Low Reynolds number mixed convection in vertical tubes with uniform heat flux. Int. J. Heat Mass Transf. 46, 4823–4833.

Choi, S.U.S., 1995. Enhancing thermal conductivity of fluid with nanoparticles. Developments and Applications of Non-Newtonian Flow, ASME, FED 231/MD 66, pp. 99–105.

Choi, S.U.S., Zhang, Z.G., Yu, W., Lockwood, F.E., Grulke, E.A., 2001. Anomalous thermal conductivity enhancement in nanotube suspensions. Appl. Phys. Lett. 79 (14), 2252–2254.

Choudhury, D., Patankar, S.V., 1988. Combined forced and free laminar convection in the entrance region of an inclined isothermal tube. J. Heat Transf. Trans. ASME 110 (4), 901–909.

Daungthongsuk, W., Wongwises, S., 2007. A critical review of convective heat transfer of nanofluids. Renew. Sust. Energy Rev. 11 (5), 797–817.

Ding, Y., Wen, D., 2005. Particle migration in a flow of nanoparticle suspensions. Powder Technol. 149, 84–92.

Estman, J.A., Choi, S.U.S., Li, S., Yu, W., Thomson, L.J., 2001. Anomalously increased effective thermal conductivities of ethylene glycol based nanofluid containing copper nanoparticles. Appl. Phys. Lett. 78, 718–720.

Hamilton, R.L., Crosser, O.K., 1962. Thermal conductivity of heterogeneous two-component system. I & EC Fundamental 1 (3), 187–191.

Keblinski, P., Phillpot, S.R., Choi, S.U.S., Eastman, J.A., 2002. Mechanisms of heat flow in suspensions of nano-sized particles (nanofluid). Int. J. Heat Mass Transf. 45, 855–863.

Khanafer, K., Vafai, K., Lightstone, M., 2003. Buoyancy-driven heat transfer enhancement in a two dimensional enclosure utilizing nanofluids. Int. J. Heat Mass Transf. 46, 3639–3653.

Koo, J., Kleinstreuer, C., 2005. Laminar nanofluid flow in microheatsinks. Int. J. Heat Mass Transfer 48, 2652–2661.

Lee, S., Choi, S.U.S., Li, S., Eastman, J.A., 1999. Measuring thermal conductivity of fluids containing oxide nanoparticles. J. Heat Transf. 121, 280–289.

Maiga, S.E., Nguyen, C.T., Galanis, N., Roy, G., 2004. Heat transfer behaviours of nanofluids in a uniformly heated tube. Super Lattices Microstruct. 35 (3-6), 543–557.

Masuda, H., Ebata, A.TeramaeK., Hishinuma, N., 1993. Alteration of thermal conductivity and viscosity of liquid by dispersing ultra-fine particles (dispersions of -Al_2O_3, SiO_2, and TiO_2 ultra-fine particles). Netsu Bussei (Japanese) 4, 227–233.

Maxwell, J.C., 1873. Electricity and Magnetism. Clarendon press, Oxford, Uk.

Nesreddine, H., Galanis, N., Nguyen, C.T., 1997. Variable-property effects in laminar aiding and opposing mixed convection of air in vertical tubes. Numer. Heat Transf. A 31 (31), 53–69.

Orfi, J., Galanis, N., Nguyen, C.T., 1988. Laminar fully developed incompressible flow with mixed convection in inclined tubes. Int. J. Numer. Meth. Heat Fluid Flow 3 (4), 901–908.

Pak, B.C., Cho, Y.I., 1998. Hydrodynamic and heat transfer study of dispersed fluids with submicron metallic oxide particles. Exp. Heat Transf. 11 (2), 151–170.

Putra, N., Roetzel, W., Das, S.K., 2003. Natural convection of nano fluids. J. Heat Mass Transf. 39, 775–784.

Sabbagh, J.A., Aziz, A., El-Ariny, A.S., Hamad, G., 1976. Combined free and forced convection in inclined circular tubes. Trans. ASME J. Heat Transf. 98 (2), 322–324.

Wang, X., Xu, X., Choi, S.U.S., 1999. Thermal conductivity of nanoparticle-fluid mixture. J. Thermophys. Heat Transf. 13 (4), 474–480.

Xuan, Y.M., Li, Q., 2000. Heat transfer enhancement of nanofluids. Int. J. Heat Fluid Flow 21, 58–64.

Xuan, Y.M., Li, Q., 2003. Investigation on convective heat transfer and flow features of nanofluids. J. Heat Transf. 125, 151–155.

Xuan, Y.M., Roetzel, W., 2000. Conceptions for heat transfer correlation of nanofluids. Int. J. Heat Mass Transf. 43 (19), 3701–3707.

Xuan, Y.M., Li, Q., Hu, W., 2004. Aggregation structure and thermal conducting of nanofluids. AIChE J. 49 (4), 1038–1043.

Xue, Q.Z., 2003. Model for effective thermal conductivity of nanofluids. Phys. Lett. A 307 (5–6), 313–317.

Yang, Y., Zhang, Z.G., Grulke, E.A., Anderson, W.B., Wu, G., 2005. Heat transfer properties of nanoparticle-in-fluid dispersions (nanofluids) in laminar flow. Int. J. Heat Mass Transf. 48 (6), 1106–1116.

Zhang, Z., Gu, H., Fujii, M., 2007. Effective thermal conductivity and thermal diffusivity of nanofluids containing spherical and cylindrical nanoparticles. Exp. Therm. Fluid Sci. 31, 5593–5599.